Speed Control of Small Motors Through the Ćuk Converter Topology

Michael Hutchins
School of Science and Engineering
University of Waikato
New Zealand

Jonathan Scott
School of Science and Engineering
University of Waikato
New Zealand

***Abstract*—The Ćuk Converter offers simultaneous buck-boost operation, but requires careful design owing to its having a fourth-order transfer function and numerous practical design constraints. We exploit a serendipitous overlap between the converter circuit and the equivalent circuit of a dc motor to design a motor controller that can operate with supply voltage that is lower than the motor full-speed requirement. We examine the transfer function when such a topology is used to control the speed of a small motor. We conclude that the approach is relatively straightforward owing to the impact of the motor's inductance. Measurements agree with theory.**

***Index Terms*—motor speed control, Cuk converter, switchmode power conversion.**

I. Introduction

A. Ćuk Converter

When Middlebrook and his graduate student Slobodan Ćuk presented in 1983 the detail of their 1977 design for a switchmode converter, the design grabbed the imagination of researchers because it approximated the "ideal dc transformer" [1]. The topology offered conversion between input and output dc voltages, with the voltage magnitude ratio set purely by the duty cycle of drive to a single switch, one side of which could be at ground potential. The outline circuit is shown in figure 1.

For a number of reasons the design was slower to take off than its promise might have lead the reader to expect. The transfer function is fourth order; the position of poles varies not only with component values, but also the controlling duty cycle; parasitic resistance in the two inductors and the so-called "Ćuk capacitor" all tend to significantly displace the poles of the characteristic equation; and the circuit was relatively complicated compared to other topologies [2]. Only now in the 21^{st} century is the converter used with any confidence. For example, modern switching methods are just being applied [3], and a search of the Xplore Digital Library yields a total of 48 papers with "Ćuk" in the title published between 1990 and 1999, but 137 papers in the decade and a half since January 2000 [4]. Along with its variant the Single-Ended Primary-Inductance Converter (SEPIC converter) that swaps the position of output switch and inductor, and is thus able to generate an output voltage of the same polarity as the input, the Ćuk converter is the most versatile, but hardest to design, of switchmode converters.

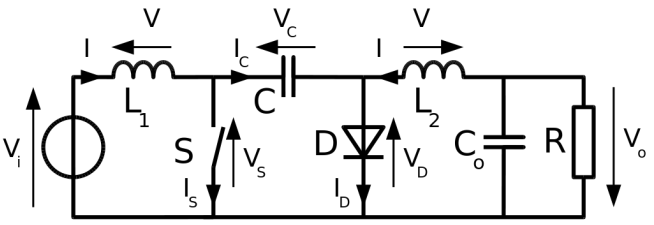

Fig. 1. Circuit of the Ćuk converter showing the conventions for currents and voltages. The middle capacitor "C" is the "Ćuk Capacitor". The switch S is usually a transistor with grounded source/emitter.

B. Brushed DC Motor

A brushed dc (BDC) motor has an equivalent circuit that consists of the series combination of a voltage source, a resistance and an inductance. The voltage source represents the energy sink that is the mechanical output of the motor, or the source of electrical energy coming from the mechanical components when the motor operates in generator mode. The I-V characteristic of this voltage source embodies the pole that arises from the mass of the mechanical components as well as the loss inherent in doing mechanical work. Previous work has shown that feedback control of the speed of small BDC motors presents greater difficulty that control of larger motors, as the mechanical pole tends not to be dominant [5].

The equivalent circuit of a BDC motor, shown in figure 2, presents 2 poles. It also bears a strong resemblance to some components of the Ćuk topology. Consider in the circuit of figure 1 that the parallel combination of C_o and R will resemble a voltage source if C_o is large, and L_2 with its inescapable parasitic resistance map exactly to L_m and R_m in figure 2. Overlaying these two circuit diagrams with the motor replacing the equivalent parts of the Ćuk circuit leads to the circuit of figure 3.

II. Transfer Function

We will now consider the transfer function of the circuit of figure 3 driving a typical, physically-small BDC motor. The mathematical derivation of the state-space equations is given in the appendix. Predictions will be made using these equations, evaluated in Matlab.

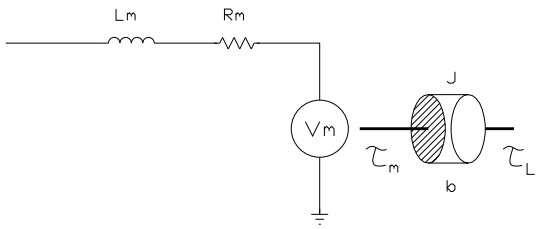

Fig. 2. The equivalent circuit of a brushed dc motor from [5].

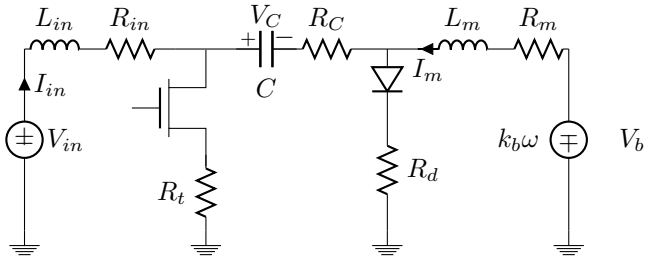

Fig. 3. The equivalent circuit of a Ćuk converter including parasitic resistances, driving a brushed dc motor that contributes L_m, R_m, and V_b. Note that V_b is proportional to the angular speed of the motor, ω.

The series inductance of a small motor is typically a few millihenries. Our example motor has $L_m = 16$mH. Motors with rotors of about 1 cubic centimetre typically have this or even smaller an inductance.

Given the ability to switch at around 100kHz, we expect values for L_{in} in the range up to a hundred μH; we will start with 10μH which is quite practical a value for small converter circuits. Practical values of the Ćuk capacitor are around a few μF; we will start with 2.2μF. We will consider at first the case where duty cycle D is 50%. Figure 4 sets the scene.

Arrows show the movement of the poles as L_m rises from a few mH to a few hundred mH. Poles 3 and 4 lie close to 40 radians/second, and figure 5 blows up this part of the plot. Pole 4 describes a small, almost-closed arc. Pole 3 nearly crosses Pole 4 as L_m moves past a value of 337mH. Figure 6 shows the movement of Pole 1 and Zero 1, which remain far out and not of much interest. It is clear that Poles 3 and 4, or rather their separation, may be of concern when applying feedback control to regulare V_b.

We next consider the variation of duty cycle, D. Motor inductance is held at 16mH, corresponding to our test motor, L_{in} is kept at 10μH and the Ćuk capacitor stays at 2.2μF. Figure 7 plots the interesting (close-in) situation. The two close poles, 3 and 4, actually separate as the duty cycle is increased, so that stability is likely to be better at higher loads. Crucially, this figure suggests that the converter-motor system will be no more difficult to control once feedback is applied than was the motor alone, that is with the motor powered with something close to an ideal voltage amplifier (or PWM equivalent).

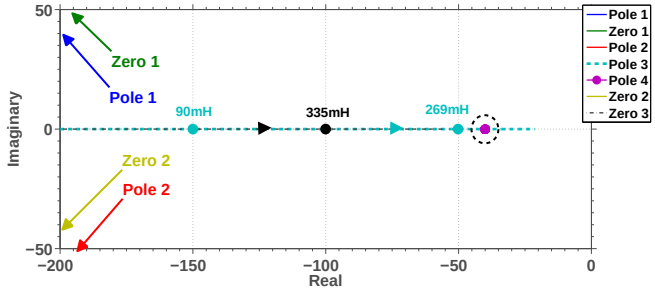

Fig. 4. The pole-zero diagram of the converter-motor combination. A complex conjugate pair of poles and a complex conjugate pair of zeroes lie ot to the left of the plot, while the dashed circle encloses a pair of poles associated with the motor components. These are expanded in figure 5.

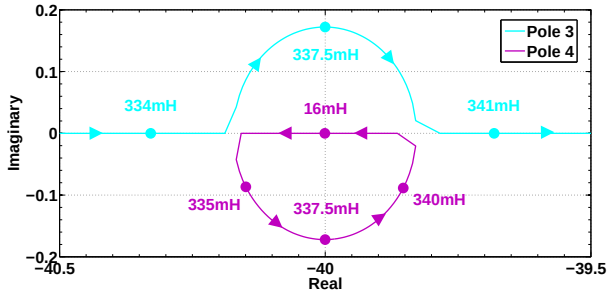

Fig. 5. The trajectory of Poles 3 and 4, the "motor inductance" and "mechanical" poles, as L_m is varied.

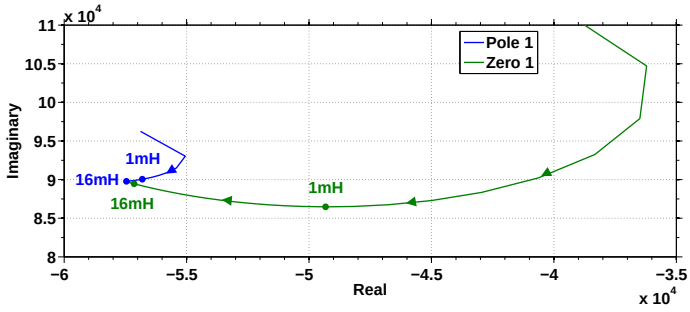

Fig. 6. The trajectory of Pole 1 and Zero 1 as L_m varies. Note the large x-axis scale.

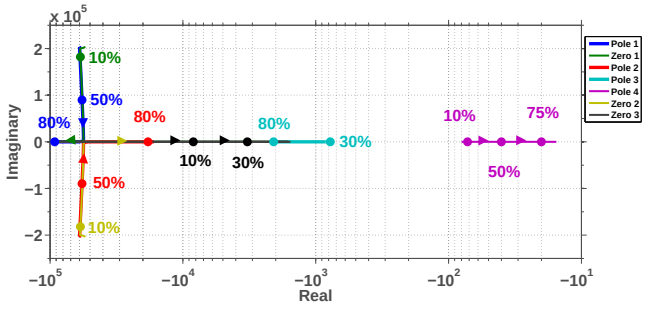

Fig. 7. Close-in pole and zero trajectories as Duty Cycle, D, is varied while other components remain at their default values. Note especially that Poles 3 & 4 *separate* as D increases, improving stability prospects as the converter increases its power transfer.

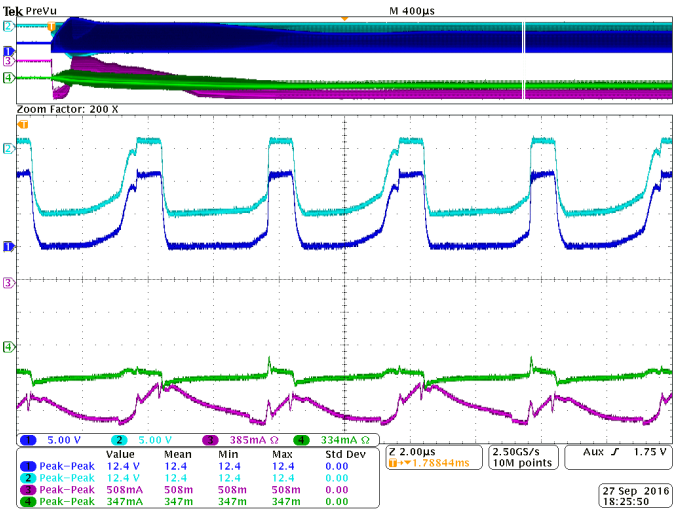

Fig. 8. Oscilloscope screen capture of the converter being subjected to a step input change in duty cycle D. The top window shows the evolution over milliseconds, the lower window the instantaneous values once the step has settled but the shaft speed has not changed. Traces show the MOSFET drain voltage, the diode voltage (with V_C being the difference of these), the input (green) and output (purple, bottom trace) current.

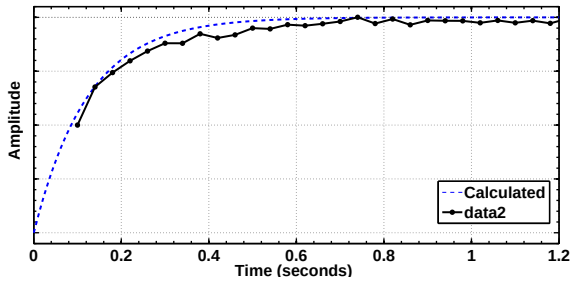

Fig. 9. Variation of shaft speed in response to a step change in D. The speed data does not extend to zero because it is measured from the period of signals from an optical encoder on the shaft and no data is available until the shaft has moved through a few degrees.

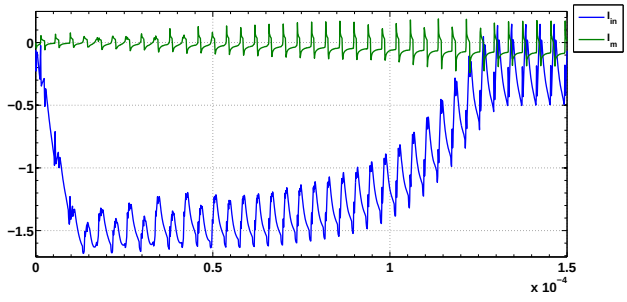

Fig. 10. Measured instantaneous input and motor current in response to a step change in D from 0 to 50%.

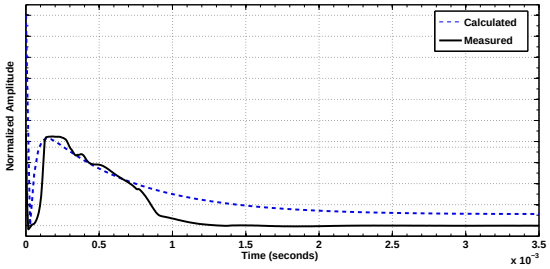

Fig. 11. Predicted and measured values of the averaged input current in response to a step input of duty cycle, D, from 0 to 50%.

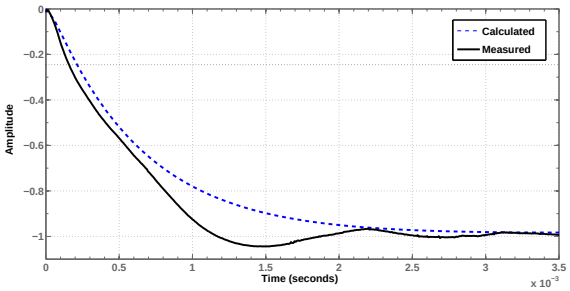

Fig. 12. Predicted and measured values of the mean output current in response to a step input of duty cycle, D, from 0 to 50%

III. Measured Results

Reassured by the above analysis of the transfer function, we construct a converter with the default values above, a 5V input supply, and a 12V BDC motor with $L_m = 16$mH series inductance and 12Ω resistance, $L_{in} = 10\mu$H, $R_{in} = 1.2\Omega$, $R_C = 0.1\Omega$, $R_t = 0.1\Omega$, $R_d = 0.1\Omega$, $J = 0.05$, $b = 0.8$, and $K_b = 0.01$.

Figure 8 is a screen capture from measurements made on the prototype. To a remarkable degree to time-domain waveforms have the instantaneous shape that is to be expected, except for finite risetimes and small "wiggles" that are attributed to measurement artefacts and extraneous parasitic impedances. The upper part of the figure shows the evolution of waveforms on a longer time scale. Figure 9 shows the variation of shaft speed on yet longer a time scale. Matlab simulation agrees with measured data where available. Figure 10 shows the input and output currents in response to the same step input. While the input inductor current may spike, the output current describes, on average, a smooth response reminiscent of a single-pole exponential change. Figures 11 and 12 show the evolution of predicted and measured mean input and output current. There is a discrepancy about 1 second that is attributed to mechanical imperfections in the apparatus and errors in our values for electrical parasitics.

IV. Conclusion

We have shown that the Ćuk topology is readily applied to drive a small motor. The overlap of circuit topologies results in poles from the motor replacing poles in the Ćuk transfer function to yield only the same number of poles (order of the system) as existed without the motor. Component values can be chosen so as to leave a dominant pole, and a system around which feedback can be applied with no more complexity than existed in the case of the motor driven by a perfect analog source.

Appendix

There are various ways to model a switchmode circuit [6]. Here we develop the state-space equations for the circuit of figure 3 [7], [8]. Including the mechanical pole of the motor and load, the system will be of fourth order. Let the state be

$$x = \begin{bmatrix} I_{in} \\ I_m \\ V_C \\ \omega \end{bmatrix} \tag{1}$$

where I_{in} is the (input) current drawn from the source through inductor L_{in}, I_m is the motor (output) current, V_C is the voltage across the Ćuk capacitor, and ω is the (desired) motor shaft output rotational speed. Next we define the input variables

$$u = \begin{bmatrix} V_{in} \\ T_L \end{bmatrix} \tag{2}$$

where V_{in} is the supply (input) voltage and T_L is the torque (load) encountered on the motor output shaft. Then

$$\dot{x} = Ax + Bu \tag{3}$$
$$y = Cx \tag{4}$$

where y is the output of the system. The state-space equations are perturbed with

$$d = D + \hat{d} \tag{5}$$
$$x = X + \hat{x} \tag{6}$$
$$y = Y + \hat{y} \tag{7}$$
$$u = U + \hat{u} \tag{8}$$

In steady state

$$\dot{x} = AX + BU = 0 \tag{9}$$
$$X = -A^{-1}BU \tag{10}$$
$$Y = CX \tag{11}$$

We have a continuous, time-varying system, as the switch has two states. The state matrix A is represented by two matrices, A_1 and A_2 representing the switch-closed and switch-open conditions. The variable D weights the two condition state matrices. Next we write

$$\dot{\hat{x}} = A\hat{x} + B\hat{u} + [(A_1 - A_2)X + (B_1 - B_2)U]\hat{d} \tag{12}$$
$$\hat{y} = C\hat{x} + (C_1 - C_2)X\hat{d} \tag{13}$$

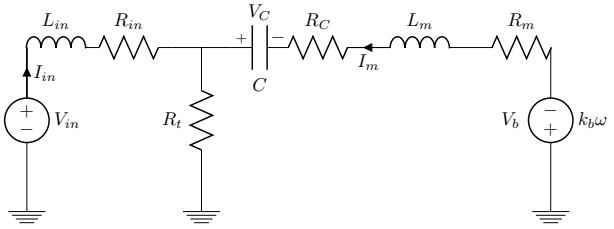

Fig. 13. Circuit with driving switch in the ON state.

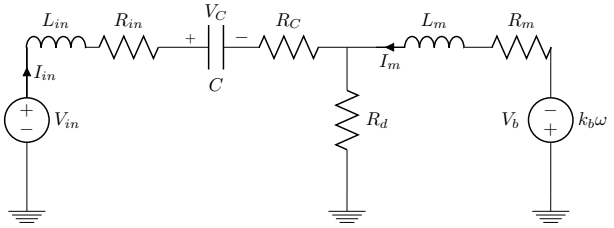

Fig. 14. Circuit with driving switch in the OFF state.

where

$$A = DA_1 + (1 - D)A_2 \tag{14}$$
$$B = DB_1 + (1 - D)B_2 \tag{15}$$
$$C = DC_1 + (1 - D)C_2 \tag{16}$$

A. On state

When the switch is closed the circuit becomes that shown in figure 13. Application of Kirchoff's laws yields:

$$\frac{dI_{in}}{dt} = \frac{1}{L_{in}}V_{in} - \frac{R_{in} + R_t}{L_{in}}I_{in} - \frac{R_t}{L_{in}}I_m \tag{17}$$
$$\frac{dI_m}{dt} = \frac{1}{L_m}V_C - \frac{k_b}{L_m}\omega - \frac{R_m + R_C + R_t}{L_m}I_m - \frac{R_t}{L_m}I_{in} \tag{18}$$
$$\frac{dV_C}{dt} = \frac{-1}{C}I_m \tag{19}$$
$$\frac{d\omega}{dt} = \frac{k_t}{J}I_m - \frac{b}{J}\omega - \frac{T_L}{J} \tag{20}$$

B. Off state

When the switch is closed the circuit becomes that shown in figure 14. Again the application of Kirchoff's laws yields:

$$\frac{dI_{in}}{dt} = \frac{1}{L_{in}}V_{in} - \frac{R_{in} + R_C + R_d}{L_{in}}I_{in} - \frac{R_d}{L_{in}}I_m - \frac{1}{L_{in}}V_C \tag{21}$$
$$\frac{dI_m}{dt} = -\frac{k_b}{L_m}\omega - \frac{R_m + R_d}{L_m}I_m - \frac{R_d}{L_m}I_{in} \tag{22}$$
$$\frac{dV_C}{dt} = \frac{1}{C}I_{in} \tag{23}$$
$$\frac{d\omega}{dt} = \frac{k_t}{J}I_m - \frac{b}{J}\omega - \frac{T_L}{J} \tag{24}$$

C. State Space Matrices

We are finally able to derive the two matrices

$$A_1 = \begin{bmatrix} -\frac{R_{in}+R_t}{L_{in}} & -\frac{R_t}{L_{in}} & 0 & 0 \\ -\frac{R_t}{L_m} & -\frac{R_m+R_C+R_t}{L_m} & \frac{1}{L_m} & -\frac{k_b}{L_m} \\ 0 & -\frac{1}{C} & 0 & 0 \\ 0 & \frac{k_t}{J} & 0 & -\frac{b}{J} \end{bmatrix} \tag{25}$$

$$A_2 = \begin{bmatrix} -\frac{R_{in}+R_C+R_d}{L_{in}} & -\frac{R_d}{L_{in}} & -\frac{1}{L_{in}} & 0 \\ -\frac{R_d}{L_m} & -\frac{R_m+R_d}{L_m} & 0 & -\frac{k_b}{L_m} \\ \frac{1}{C} & 0 & 0 & 0 \\ 0 & \frac{k_t}{J} & 0 & -\frac{b}{J} \end{bmatrix} \tag{26}$$

and

$$B = B_1 = B_2 = \begin{bmatrix} \frac{1}{L_{in}} & 0 \\ 0 & 0 \\ 0 & 0 \\ 0 & \frac{T_L}{J} \end{bmatrix} \tag{27}$$

$$C = C_1 = C_2 = \begin{bmatrix} 0 & 0 & 0 & 1 \end{bmatrix} \tag{28}$$

which will permit calculation of the performance of the circuit using a tool such as Matlab.

REFERENCES

[1] Slobodan Cuk, and R. D. Middlebrook, "Advances in Switched-Mode Power Conversion Part I," *IEEE Transactions on Industrial Electronics*, Vol. IE-30, no. 1, pp10–19, 1983.

[2] B. Bryant and M. K. Kazimierczuk, "Derivation of the Ćuk PWM DC-DC converter circuit topology", *Proceedings of the 2003 International Symposium on Circuits and Systems*, ISCAS '03, vol. 3, ppIII-292–III-295.

[3] B-R. Lin, C-L. Huang and J-F. Wan, "Analysis of a Zero Voltage Switching Cuk Converter", 33rd Annual Conference of the IEEE Industrial Electronics Society, IECON 2007, pp1972–1977.

[4] IEEE Xplore digital library, http://ieeexplore.ieee.org/, searched October 2016.

[5] John McLeish, Howell Round, and Jonathan Scott, "Speed Control with Low Armature Loss for Very Small Sensorless Brushed DC Motors", *IEEE Transactions on Industrial Electronics*, Vol 56, no. 4, April 2009, pp1223–1229.

[6] P. R. K. Chetty, "Modelling and Analysis of Ćuk Converter Using Current Injected Equivalent Circuit Approach," *IEEE Transactions on Industrial Electronics*, Vol IE-30, no. 1, February 1983, pp56–59.

[7] W. M. Polivka, P. R. K. Chetty, and R. D. Middlebrook, "State-Space Average modelling of converters with parasitics and storage-time modulation," *IEEE Power Electronics Specialists Conference*, June 1980.

[8] G.F. Franklin, J.D. Powell and A. Emami-Naeini, *Feedback Control of Dynamic Systems*, 7th Edition, Pearson, 2015.